—Supporting Information—

Novel Solar Cell Materials: Insights From First Principles

[1]Gopalakrishnan Sai Gautam, [1,†]Thomas P. Senftle, [2,¶]Nima Alidoust, and [3,*]Emily A. Carter

[1]Department of Mechanical and Aerospace Engineering, [2]Department of Electrical Engineering, and [3]School of Engineering and Applied Science,
Princeton University, Princeton, NJ 08544-5263, United States
*Corresponding author, e-mail: eac@princeton.edu
[†] Present address: Department of Chemical and Biomolecular Engineering, Rice University, Houston, TX 77005
[¶]Present address: Rigetti Computing, 2919 7th Street, Berkeley, CA 94710

Overview of theoretical methods

The studies summarized in the manuscript utilize a variety of theories, a brief overview of which is given below. A detailed discussion on appropriate approximations to invoke in solid-state QM calculations can be found in the reviews by Bendavid and Carter,[1] Cramer and Truhlar,[2] and Harvey.[3] Examples of how QM calculations can be used to describe TMOs and their alloys for allied phenomena such as photocatalysis can be found in the review by Liao and Carter,[4] and Le Bahers *et al*.[5]

Bulk energies

A variety of approximations within the general framework of the density functional theory (DFT)[6,7] can be used for quantitative or qualitative evaluation of energetic and electronic properties, including the systems of interest in this review, *i.e.*, pure, doped, or alloyed NiO, CoO, FeO, Cu_2O, and Cu_2ZnSnS_4 (CZTS).[8–12] The most important term that dictates the accuracy of DFT calculations is the choice of the necessarily approximate exchange-correlation (XC) functional.[13] Common XC functionals for condensed matter include the local density approximation (LDA)[14,15] and the Perdew-Burke-Ernzerhof (PBE) implementation of the generalized gradient approximation (GGA).[16] The strongly constrained appropriately normed

(SCAN) functional[17] introduced recently was shown to satisfy all 17 known constraints for the behavior of an XC functional, unlike the GGA or the LDA,[13] a truly impressive achievement. Gautam *et al.*[12] therefore employed SCAN to understand the influence of dopants on defect energetics in CZTS. Although SCAN is formally very appealing, density of states (DOS) calculations in CZTS[12] reveal that SCAN still exhibits the typical failure of pure density functionals: it fails to reproduce experimental band gaps. The lack of a derivative discontinuity in all pure density XC functionals is the source of this error.[18]

Pure DFT approximations, especially the LDA and the GGA, suffer from self-interaction errors (SIE),[15] owing to an inaccurate description of electron exchange interactions. Consequently, such approximations often fail to reproduce ground-state properties such as formation energies and lattice parameters,[19–24] especially in open-shell, transition-metal compounds.[25] Additionally, as a ground-state theory, pure DFT approximations usually underestimate band gaps of semiconductors.[26,27] Prior studies have shown that either adding a Hubbard U correction to the DFT Hamiltonian (resulting in a DFT+U framework)[28,29] or incorporating some exact exchange from Hartree-Fock (HF) theory via hybrid functionals (*e.g.*, Heyd-Scuseria-Ernzerhof, HSE[30] or PBE0[31]) often yield better quantitative estimations of formation energies and qualitative predictions of band gaps. Specifically, DFT+U has the advantage of not adding significant computational cost to a DFT calculation, unlike hybrid functionals in periodic planewave basis calculations that can be two orders of magnitude more expensive.[30] However, the magnitude of U is not known *a priori* and must be separately determined and validated, preferably by *ab initio* approaches.[32–35] Hence, the DFT+U framework, among others, was used to study the bulk stability of all the TMO systems reviewed in the main text (NiO, CoO, FeO, and Cu_2O). The specific U values employed on the transition metal centers are also indicated within the appropriate sections

of the main text. Interestingly, based on benchmarking SCAN and experimental formation energies of binary sulfides, Gautam *et al.*[12] concluded that a +*U* correction with SCAN was not required to accurately describe the ground-state properties of CZTS.

Band gaps

For quantitative comparisons of calculated band gaps with experiments, a ground-state theory, such as DFT, DFT+*U*, hybrid DFT (e.g., HSE), is not of much utility since the unoccupied virtual bands (*i.e.*, conduction bands) are not described accurately. Thus, advanced excited-state methods, such as the many-body Green's function theory (GW),[36,37] are often employed for this purpose. Notably, GW theory provides a framework to calculate the self-energy of a many-electron system via an expansion of the single-particle Green's function (G) that describes the propagation of an electron within a screened Coulombic potential (W). Physically, the GW approximation is equivalent to adding a "dynamically screened" Coulomb potential[38] to DFT.

Although self-consistent GW calculations can be performed, prior studies have shown that doing a non-self-consistent GW calculation (G_0W_0)[39] as a perturbation to the ground-state one-electron wavefunctions and eigenvalues obtained from DFT (*i.e.*, DFT+G_0W_0) often yields accurate band gaps even in small-gap semiconductors.[40–43] G_0W_0 calculates a quasiparticle (QP) band gap directly comparable to a measured photoemission/inverse photoemission gap. The accuracy of G_0W_0 calculations, however, relies on the quality of the ground-state wavefunctions obtained from DFT and the use of a sufficient number of virtual states to obtain a reliable band gap.[44] Since DFT+*U* provides a better description of ground-state wavefunctions in open-shell systems, DFT+*U*+G_0W_0 calculations can furnish accurate predictions of transition-metal oxide band gaps.[45,46] Thus, based on benchmarking theoretical predictions with experiments, Alidoust and Carter[10,47] used PBE+*U*+G_0W_0 and LDA+*U*+G_0W_0 for band-gap calculations in (pure and

doped) NiO and CoO, respectively, where the magnitude of U values used for Ni and Co were obtained from size-converged electrostatically embedded unrestricted HF calculations.[48,49]

Charge transfer barriers

Charge transport in transition metal oxides is most often best described by using the small polaron model.[50,51] A small polaron is the combination of a localized carrier (hole or electron) and a localized lattice distortion that affects a few surrounding ions (distances less than the lattice constant) from the localized carrier.[50–54] In the case of (pure, doped, and alloyed) NiO and FeO, as modeled by Alidoust and Carter,[55,56] and Toroker and Carter,[57] respectively, a small hole polaron is predicted to form when a hole localizes on an oxygen in NiO (*i.e.*, forming O^{1-} from O^{2-}) and *via* hole localization on an iron in FeO (*i.e.*, forming the stable, half-filled *d*-shell Fe^{3+} from Fe^{2+}). These are the most stable positions of the hole, as opposed to forming Ni^{3+} or O^{-1} in NiO and FeO, respectively. Hole polarons can migrate within a lattice from a donor (O^{1-} in NiO and Fe^{3+} in FeO) to an acceptor site (O^{2-} in NiO, Fe^{2+} in FeO), limited by a barrier ΔG^*, which can be estimated using the Marcus theory of electron transfer (*vide infra*).[58,59]

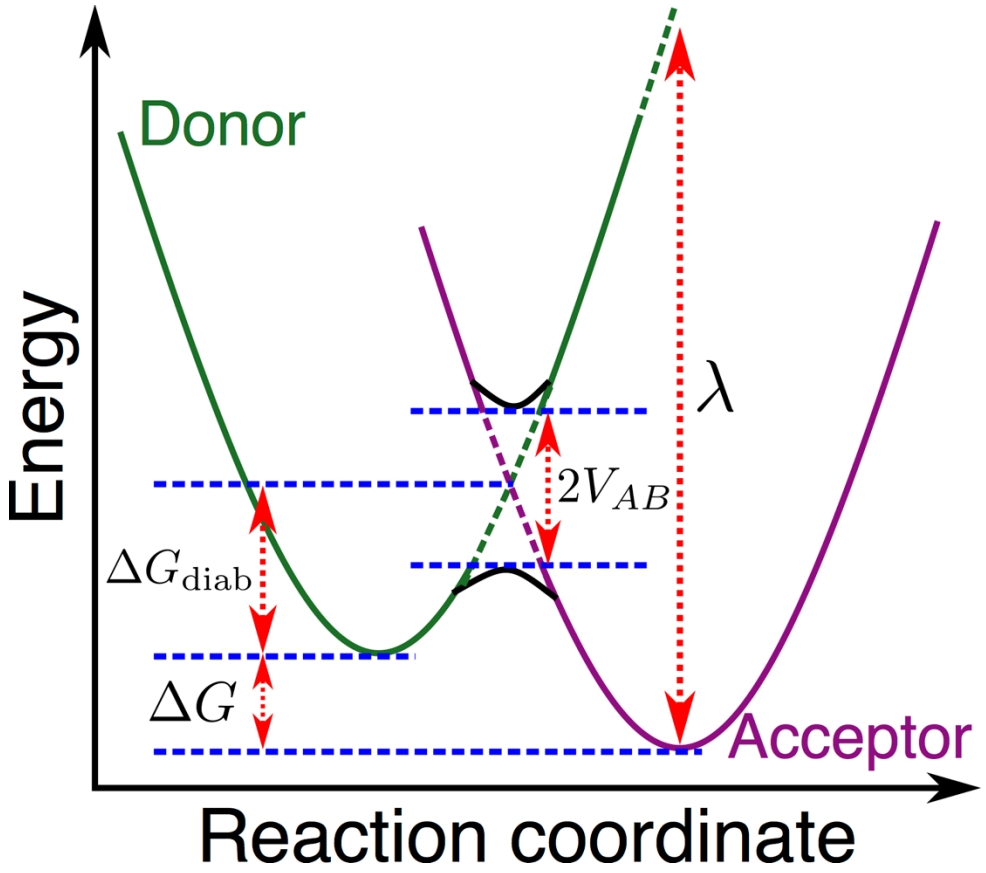

Figure S1: Schematic of potential energy surfaces during CT within the framework of Marcus theory.[58]

Figure S1 displays a schematic of a parabolic potential energy surface (within the framework of Marcus theory) around a donor (D, green curve) site and an acceptor (A, purple) site during charge (*e.g.*, hole polaron) transfer in a material. Note that the donor and acceptor states are defined by a set of collective nuclear coordinates, q_{D} and q_{A}, respectively, and the free energy difference between the two states is given by ΔG in **Figure S1**. If the potential energy surfaces are known for the donor and acceptor states, then one can calculate a reorganization energy (λ in **Figure S1**) as the energy required to distort the lattice from the equilibrium configuration of the donor $(q_{\mathrm{D}})_{\mathrm{equil}}$ to the equilibrium configuration of the acceptor $(q_{\mathrm{A}})_{\mathrm{equil}}$ without the hole (or electron) being transferred. The actual CT process can occur under two distinct scenarios:[58] *i*) the donor and acceptor nuclei do not move when the charge is transferred, *i.e.*, nuclear and charge

motion are decoupled, referred to as the "diabatic" approximation; and *ii*) both the donor and acceptor move during CT, *i.e.*, the nuclei and charge motion are highly coupled, referred to as the "adiabatic" approximation.

In the diabatic CT scenario (dashed and solid green and purple lines in **Figure S1**), the transferring charge has to "jump" from the donor energy surface to the acceptor energy surface at the crossing point (q_c), *i.e.*, the point of intersection between the green and purple dashed lines in **Figure S1**. In the case of adiabatic CT (solid black curves), the potential energy curves split into distinct ground- and excited-state configurations at q_c, where the extent of coupling between the donor and acceptor energy curves is quantified via the coupling matrix element, V_{AB}. Note that the energy difference between the ground- and excited-state configurations at q_c (ΔE) is twice that of the coupling matrix element, *i.e.*, $\Delta E = 2V_{AB}$.

In general, $\Delta G^*$for CT from the donor to the acceptor (D→A), given λ and V_{AB}, can be expressed as $\Delta G^* = -\frac{\lambda}{4} + \frac{(\lambda^2+4V_{AB}^2)^{\frac{1}{2}}}{2} - V_{AB}$,[60] where the CT barrier for A→D is $\Delta G^* + \Delta G$. Under the diabatic approximation, $V_{AB} \approx 0$, and $\Delta G^* = \Delta G_{diab} \sim \frac{\lambda}{4}$, which signifies that the barrier can be efficiently calculated if the ground-state energy curves of the donor and acceptor states are known (computed via robust, self-consistent, ground-state methods). In contrast, under the adiabatic approximation $\left(0 < V_{AB} \ll \frac{\lambda}{2}\right)$, ΔG^* reduces from ΔG_{diab} by approximately the coupling element, *i.e.*, $\Delta G^* = \Delta G_{adiab} \sim \frac{\lambda}{4} - V_{AB}$,[61] necessitating the explicit evaluation of both the ground- and excited-state energies at q_c. It is difficult to determine *a priori* if ΔG_{adiab} is substantially different from ΔG_{diab} for a given material. Hence, performing a few representative calculations of V_{AB} to verify the (a)diabatic nature of CT is recommended.[55]

Following previous theoretical work[54,62,63] calculating polaron migration barriers in pure and doped TMOs, Alidoust and Carter[55,56] and Toroker and Carter[57] estimated the diabatic barriers (ΔG^*_{diab}) in NiO and FeO, respectively, using structurally relaxed unrestricted Hartree-Fock (UHF[64]) calculations on electrostatically embedded clusters. Carved out of rocksalt NiO (FeO) periodic crystals, the clusters were capped with Mg effective core potentials (ECPs)[65] to compensate for missing Ni^{2+} (Fe^{2+}) ions adjacent to O^{2-} and to account for Pauli repulsion between cluster electrons and neighboring core electrons of the +2 ions. The ECP-capped cluster was then embedded within an aperiodic point charge array to represent the electrostatic potential arising from the surrounding crystal structure.[66] The intermediate states were obtained via the linear coordinate approximation after optimizing the geometry of the donor and acceptor hole configurations.[67]

To calculate the adiabatic hole transfer barrier in NiO, Alidoust and Carter[55,56] employed complete active space self-consistent field (CASSCF) calculations[68] to evaluate the excited-state energy. Note that a single-determinant, ground-state theory, such as UHF, cannot accurately describe the coupled wavefunctions (and the consequent split in energy levels) at the transition state. The computationally expensive CASSCF calculations instead includes all possible excited state configurations within a subspace (called the active space) in its wavefunction, along with a self-consistent optimization of the orbital shapes that give rise to those configurations.

Lattice disorder

Lattice disorder, or any order-disorder phase transformation in a given solid, can be described via a cluster expansion (CE[69]) model. A CE is a generalized Ising model[70] that describes the total energy of a given lattice in terms of atomic occupations over various lattice sites. In practice, CE

models are often written as a truncated series of cluster interactions, such as interactions between pairs, triplets, *etc.*[71] The truncated series then is fit to an input set of configurations (typically built from the supercells of a given structure) and their corresponding energies (calculated *via* DFT or a similar theory). In combination with canonical Monte Carlo (MC) simulations, where the CE evaluates the energy during each MC sweep, CE models can be used to estimate the configurational entropy of a lattice and have been shown to accurately estimate order-disorder transitions.[72–74]

To investigate the origins of disorder within the CZTS structure (in other words, to probe the order-disorder transition within CZTS), Yu and Carter[11,75] performed MC simulations based on a CE model built on a set of PBE+*U* calculations in CZTS. The *U* values of Cu, Zn, and Sn used in the PBE+*U* calculations were determined from previous electrostatically embedded unrestricted HF calculations.[35] To construct the CE, the authors[75] considered four different pair and triplet interactions. Note that Yu and Carter[11,75,76] also added long-range dispersion corrections, namely Grimme's *a posteriori D2* correction,[77] in all of their PBE+*U* calculations (resulting in a PBE+*U*+*D2* functional) to improve predictions of the lattice constants and the bulk modulus.[76]

References

(1) Bendavid, L. I.; Carter, E. A. Status in Calculating Electronic Excited States in Transition Metal Oxides from First Principles. In *First Principles Approaches to Spectroscopic Properties of Complex Materials*; Di Valentin, C., Botti, S., Cococcioni, M., Eds.; Springer Berlin Heidelberg, 2014; pp 47–98.

(2) Cramer, C. J.; Truhlar, D. G. Density Functional Theory for Transition Metals and Transition Metal Chemistry. *Phys. Chem. Chem. Phys.* **2009**, *11*, 10757.

(3) Harvey, J. N. On the Accuracy of Density Functional Theory in Transition Metal Chemistry. *Annu. Reports Sect. "C" Physical Chem.* **2006**, *102*, 203.

(4) Liao, P.; Carter, E. A. New Concepts and Modeling Strategies to Design and Evaluate Photo-Electro-Catalysts Based on Transition Metal Oxides. *Chem. Soc. Rev.* **2013**, *42*, 2401–2422.

(5) Le Bahers, T.; Rérat, M.; Sautet, P. Semiconductors Used in Photovoltaic and Photocatalytic Devices: Assessing Fundamental Properties from DFT. *J. Phys. Chem. C* **2014**, *118*, 5997–6008.

(6) Hohenberg, P.; Kohn, W. Inhomogeneous Electron Gas. *Phys. Rev.* **1964**, *136*, B864–B871.

(7) Kohn, W.; Sham, L. J. Self-Consistent Equations Including Exchange and Correlation Effects. *Phys. Rev.* **1965**, *140*, A1133–A1138.

(8) Isseroff, L. Y.; Carter, E. A. Electronic Structure of Pure and Doped Cuprous Oxide with Copper Vacancies: Suppression of Trap States. *Chem. Mater.* **2013**, *25*, 253–265.

(9) Toroker, M. C.; Carter, E. A. Transition Metal Oxide Alloys as Potential Solar Energy Conversion Materials. *J. Mater. Chem. A* **2013**, *1*, 2474.

(10) Alidoust, N.; Lessio, M.; Carter, E. A. Cobalt (II) Oxide and Nickel (II) Oxide Alloys as Potential Intermediate-Band Semiconductors: A Theoretical Study. *J. Appl. Phys.* **2016**, *119*, 025102.

(11) Yu, K.; Carter, E. A. Elucidating Structural Disorder and the Effects of Cu Vacancies on the Electronic Properties of Cu2ZnSnS4. *Chem. Mater.* **2016**, *28*, 864–869.

(12) Sai Gautam, G.; Senftle, T. P.; Carter, E. A. Understanding the Effects of Cd and Ag Doping in Cu 2 ZnSnS 4 Solar Cells. *Chem. Mater.* **2018**, *30*, 4543–4555.

(13) Car, R. Density Functional Theory: Fixing Jacob's Ladder. *Nat. Chem.* **2016**, *8*, 820–821.

(14) Perdew, J. P. Orbital Functional for Exchange and Correlation: Self-Interaction Correction to the Local Density Approximation. *Chem. Phys. Lett.* **1979**, *64*, 127–130.

(15) Perdew, J. P.; Zunger, A. Self-Interaction Correction to Density-Functional Approximations for Many-Electron Systems. *Phys. Rev. B* **1981**, *23*, 5048–5079.

(16) Perdew, J. P.; Burke, K.; Ernzerhof, M. Generalized Gradient Approximation Made Simple. *Phys. Rev. Lett.* **1996**, *77*, 3865–3868.

(17) Sun, J.; Ruzsinszky, A.; Perdew, J. P. Strongly Constrained and Appropriately Normed Semilocal Density Functional. *Phys. Rev. Lett.* **2015**, *115*, 036402.

(18) Perdew, J. P.; Yang, W.; Burke, K.; Yang, Z.; Gross, E. K. U.; Scheffler, M.; Scuseria, G. E.; Henderson, T. M.; Zhang, I. Y.; Ruzsinszky, A.; et al. Understanding Band Gaps of Solids in Generalized Kohn–Sham Theory. *Proc. Natl. Acad. Sci.* **2017**, *114*, 2801–2806.

(19) Broqvist, P.; Grönbeck, H.; Panas, I. Surface Properties of Alkaline Earth Metal Oxides. *Surf. Sci.* **2004**, *554*, 262–271.

(20) Milman, V.; Winkler, B.; Probert, M. I. J. Stiffness and Thermal Expansion of ZrB 2 : An Ab Initio Study. *J.*

Phys. Condens. Matter **2005**, *17*, 2233–2241.

(21) van de Walle, A.; Ceder, G. Correcting Overbinding in Local-Density-Approximation Calculations. *Phys. Rev. B* **1999**, *59*, 14992–15001.

(22) Mayor-López, M. .; Weber, J. DFT Calculations of the Binding Energy of Metallocenes. *Chem. Phys. Lett.* **1997**, *281*, 226–232.

(23) Sai Gautam, G.; Hari Kumar, K. C. Elastic, Thermochemical and Thermophysical Properties of Rock Salt-Type Transition Metal Carbides and Nitrides: A First Principles Study. *J. Alloys Compd.* **2014**, *587*, 380–386.

(24) Nørskov, J. K.; Rossmeisl, J.; Logadottir, A.; Lindqvist, L.; Kitchin, J. R.; Bligaard, T.; Jónsson, H. Origin of the Overpotential for Oxygen Reduction at a Fuel-Cell Cathode. *J. Phys. Chem. B* **2004**, *108*, 17886–17892.

(25) Wang, L.; Maxisch, T.; Ceder, G. Oxidation Energies of Transition Metal Oxides within the GGA + U Framework. *Phys. Rev. B* **2006**, *73*, 195107.

(26) Freysoldt, C.; Grabowski, B.; Hickel, T.; Neugebauer, J.; Kresse, G.; Janotti, A.; Van de Walle, C. G. First-Principles Calculations for Point Defects in Solids. *Rev. Mod. Phys.* **2014**, *86*, 253–305.

(27) Lany, S.; Zunger, A. Assessment of Correction Methods for the Band-Gap Problem and for Finite-Size Effects in Supercell Defect Calculations: Case Studies for ZnO and GaAs. *Phys. Rev. B* **2008**, *78*, 235104.

(28) Anisimov, V. I.; Zaanen, J.; Andersen, O. K. Band Theory and Mott Insulators: Hubbard U Instead of Stoner I. *Phys. Rev. B* **1991**, *44*, 943–954.

(29) Anisimov, V. I.; Aryasetiawan, F.; Lichtenstein, A. I. First-Principles Calculations of the Electronic Structure and Spectra of Strongly Correlated Systems: The LDA + U Method. *J. Phys. Condens. Matter* **1997**, *9*, 767–808.

(30) Heyd, J.; Scuseria, G. E.; Ernzerhof, M. Hybrid Functionals Based on a Screened Coulomb Potential. *J. Chem. Phys.* **2003**, *118*, 8207–8215.

(31) Adamo, C.; Barone, V. Toward Reliable Density Functional Methods without Adjustable Parameters: The PBE0 Model. *J. Chem. Phys.* **1999**, *110*, 6158–6170.

(32) Mosey, N. J.; Liao, P.; Carter, E. A. Rotationally Invariant Ab Initio Evaluation of Coulomb and Exchange Parameters for DFT+U Calculations. *J. Chem. Phys.* **2008**, *129*, 014103.

(33) Mosey, N. J.; Carter, E. A. Ab Initio Evaluation of Coulomb and Exchange Parameters for DFT + U Calculations. *Phys. Rev. B* **2007**, *76*, 155123.

(34) Cococcioni, M.; de Gironcoli, S. Linear Response Approach to the Calculation of the Effective Interaction Parameters in the LDA+U Method. *Phys. Rev. B* **2005**, *71*, 035105.

(35) Yu, K.; Carter, E. A. Communication: Comparing Ab Initio Methods of Obtaining Effective U Parameters for Closed-Shell Materials. *J. Chem. Phys.* **2014**, *140*, 121105.

(36) Onida, G.; Reining, L.; Rubio, A. Electronic Excitations: Density-Functional versus Many-Body Green's-Function Approaches. *Rev. Mod. Phys.* **2002**, *74*, 601–659.

(37) Hybertsen, M. S.; Louie, S. G. First-Principles Theory of Quasiparticles: Calculation of Band Gaps in Semiconductors and Insulators. *Phys. Rev. Lett.* **1985**, *55*, 1418–1421.

(38) Aryasetiawan, F. Self-Energy of Ferromagnetic Nickel in the GW Approximation. *Phys. Rev. B* **1992**, *46*, 13051–13064.

(39) Li, X.-Z.; Gómez-Abal, R.; Jiang, H.; Ambrosch-Draxl, C.; Scheffler, M. Impact of Widely Used Approximations to the G0W0 Method: An All-Electron Perspective. *New J. Phys.* **2012**, *14*, 023006.

(40) Gatti, M.; Bruneval, F.; Olevano, V.; Reining, L. Understanding Correlations in Vanadium Dioxide from First Principles. *Phys. Rev. Lett.* **2007**, *99*, 266402.

(41) Karlický, F.; Otyepka, M. Band Gaps and Optical Spectra of Chlorographene, Fluorographene and Graphane from G 0 W 0 , GW 0 and GW Calculations on Top of PBE and HSE06 Orbitals. *J. Chem. Theory Comput.* **2013**, *9*, 4155–4164.

(42) Cheiwchanchamnangij, T.; Lambrecht, W. R. L. Quasiparticle Band Structure Calculation of Monolayer, Bilayer, and Bulk MoS_2. *Phys. Rev. B* **2012**, *85*, 205302.

(43) Miyake, T.; Zhang, P.; Cohen, M. L.; Louie, S. G. Quasiparticle Energy of Semicore d Electrons in ZnS: Combined LDA+U and GW Approach. *Phys. Rev. B - Condens. Matter Mater. Phys.* **2006**, *74*, 245213.

(44) Samsonidze, G.; Jain, M.; Deslippe, J.; Cohen, M. L.; Louie, S. G. Simple Approximate Physical Orbitals for GW Quasiparticle Calculations. *Phys. Rev. Lett.* **2011**, *107*, 186404.

(45) Isseroff, L. Y.; Carter, E. A. Importance of Reference Hamiltonians Containing Exact Exchange for Accurate One-Shot GW Calculations of Cu2O. *Phys. Rev. B* **2012**, *85*, 235142.

(46) Liao, P.; Carter, E. A. Testing Variations of the GW Approximation on Strongly Correlated Transition Metal Oxides: Hematite (α-Fe2O3) as a Benchmark. *Phys. Chem. Chem. Phys.* **2011**, *13*, 15189.

(47) Alidoust, N.; Toroker, M. C.; Carter, E. A. Revisiting Photoemission and Inverse Photoemission Spectra of Nickel Oxide from First Principles: Implications for Solar Energy Conversion. *J. Phys. Chem. B* **2014**, *118*, 7963–7971.

(48) Alidoust, N.; Toroker, M. C.; Keith, J. A.; Carter, E. A. Significant Reduction in NiO Band Gap Upon Formation of Li x Ni 1− x O Alloys: Applications To Solar Energy Conversion. *ChemSusChem* **2014**, *7*, 195–201.

(49) Ritzmann, A. M.; Pavone, M.; Muñoz-García, A. B.; Keith, J. A.; Carter, E. A. Ab Initio DFT+U Analysis of Oxygen Transport in LaCoO3 : The Effect of Co3+ Magnetic States. *J. Mater. Chem. A* **2014**, *2*, 8060–8074.

(50) Holstein, T. Studies of Polaron Motion. *Ann. Phys. (N. Y).* **1959**, *8*, 325–342.

(51) Holstein, T. Studies of Polaron Motion. *Ann. Phys. (N. Y).* **1959**, *8*, 343–389.

(52) Kolber, M. A.; MacCrone, R. K. Bound-Polaron Hopping in NiO. *Phys. Rev. Lett.* **1972**, *29*, 1457–1461.

(53) Rosso, K. M.; Smith, D. M. A.; Dupuis, M. An Ab Initio Model of Electron Transport in Hematite (α-Fe2O3) Basal Planes. *J. Chem. Phys.* **2003**, *118*, 6455–6466.

(54) Liao, P.; Carter, E. A. Hole Transport in Pure and Doped Hematite. *J. Appl. Phys.* **2012**, *112*, 013701.

(55) Alidoust, N.; Carter, E. A. First-Principles Assessment of Hole Transport in Pure and Li-Doped NiO. *Phys. Chem. Chem. Phys.* **2015**, *17*, 18098–18110.

(56) Alidoust, N.; Carter, E. A. Three-Dimensional Hole Transport in Nickel Oxide by Alloying with MgO or ZnO. *J. Appl. Phys.* **2015**, *118*, 185102.

(57) Toroker, M. C.; Carter, E. A. Hole Transport in Nonstoichiometric and Doped Wüstite. *J. Phys. Chem. C* **2012**, *116*, 17403–17413.

(58) Marcus, R. A. Electron Transfer Reactions in Chemistry. Theory and Experiment. *Rev. Mod. Phys.* **1993**, *65*, 599–610.

(59) Marcus, R. A. Electron Transfer Reactions in Chemistry: Theory and Experiment (Nobel Lecture). *Angew. Chemie Int. Ed. English* **1993**, *32*, 1111–1121.

(60) Iordanova, N.; Dupuis, M.; Rosso, K. M. Charge Transport in Metal Oxides: A Theoretical Study of Hematite α-Fe2O3. *J. Chem. Phys.* **2005**, *122*, 144305.

(61) Kerisit, S.; Rosso, K. M. Charge Transfer in FeO: A Combined Molecular-Dynamics and Ab Initio Study. *J. Chem. Phys.* **2005**, *123*, 224712.

(62) Liao, P.; Toroker, M. C.; Carter, E. A. Electron Transport in Pure and Doped Hematite. *Nano Lett.* **2011**, *11*, 1775–1781.

(63) Kanan, D. K.; Carter, E. A. Ab Initio Study of Electron and Hole Transport in Pure and Doped MnO and MnO:ZnO Alloy. *J. Mater. Chem. A* **2013**, *1*, 9246.

(64) Amos, T.; Snyder, L. C. Unrestricted Hartree—Fock Calculations. I. An Improved Method of Computing Spin Properties. *J. Chem. Phys.* **1964**, *41*, 1773–1783.

(65) Wadt, W. R.; Hay, P. J. Ab Initio Effective Core Potentials for Molecular Calculations. Potentials for Main Group Elements Na to Bi. *J. Chem. Phys.* **1985**, *82*, 284–298.

(66) Kanan, D. K.; Sharifzadeh, S.; Carter, E. A. Quantum Mechanical Modeling of Electronic Excitations in Metal Oxides: Magnesia as a Prototype. *Chem. Phys. Lett.* **2012**, *519–520*, 18–24.

(67) Farazdel, A.; Dupuis, M.; Clementi, E.; Aviram, A. Electric-Field Induced Intramolecular Electron Transfer in Spiro .Pi.-Electron Systems and Their Suitability as Molecular Electronic Devices. A Theoretical Study. *J. Am. Chem. Soc.* **1990**, *112*, 4206–4214.

(68) Roos, B. O. The Complete Active Space SCF Method in a Fock-Matrix-Based Super-CI Formulation. *Int. J. Quantum Chem.* **1980**, *18*, 175–189.

(69) Sanchez, J.; Ducastelle, F.; Gratias, D. Generalized Cluster Description of Multicomponent Systems. *Phys. A Stat. Mech. its Appl.* **1984**, *128*, 334–350.

(70) Van Baal, C. M. Order-Disorder Transformations in a Generalized Ising Alloy. *Physica* **1973**, *64*, 571–586.

(71) Ceder, G. A Derivation of the Ising Model for the Computation of Phase Diagrams. *Comput. Mater. Sci.* **1993**, *1*, 144–150.

(72) Ceder, G.; Van der Ven, A. Phase Diagrams of Lithium Transition Metal Oxides: Investigations from First Principles. *Electrochim. Acta* **1999**, *45*, 131–150.

(73) Sai Gautam, G.; Canepa, P.; Abdellahi, A.; Urban, A.; Malik, R.; Ceder, G. The Intercalation Phase Diagram of Mg in V2O5 from First Principles. *Chem. Mater.* **2015**, *27*, 3733–3742.

(74) Zhou, F.; Maxisch, T.; Ceder, G. Configurational Electronic Entropy and the Phase Diagram of Mixed-Valence Oxides: The Case of Li_{x}FePO_{4}. *Phys. Rev. Lett.* **2006**, *97*, 155704.

(75) Yu, K.; Carter, E. A. Determining and Controlling the Stoichiometry of Cu2ZnSnS4 Photovoltaics: The Physics and Its Implications. *Chem. Mater.* **2016**, *28*, 4415–4420.

(76) Yu, K.; Carter, E. A. A Strategy to Stabilize Kesterite CZTS for High-Performance Solar Cells. *Chem. Mater.* **2015**, *27*, 2920–2927.

(77) Grimme, S. Semiempirical GGA-Type Density Functional Constructed with a Long-Range Dispersion Correction. *J. Comput. Chem.* **2006**, *27*, 1787–1799.